Causal Discovery with Reinforcement Learning

Anonymous authors
Paper under double-blind review

Abstract

Discovering causal structure among a set of variables is a fundamental problem in many empirical sciences. Traditional score-based casual discovery methods rely on various local heuristics to search for a Directed Acyclic Graph (DAG) according to a predefined score function. While these methods, e.g., greedy equivalence search, may have attractive results with infinite samples and certain model assumptions, they are less satisfactory in practice due to finite data and possible violation of assumptions. Motivated by recent advances in neural combinatorial optimization, we propose to use Reinforcement Learning (RL) to search for the DAG with the best scoring. Our encoder-decoder model takes observable data as input and generates graph adjacency matrices that are used to compute rewards. The reward incorporates both the predefined score function and two penalty terms for enforcing acyclicity. In contrast with typical RL applications where the goal is to learn a policy, we use RL as a search strategy and our final output would be the graph, among all graphs generated during training, that achieves the best reward. We conduct experiments on both synthetic and real datasets, and show that the proposed approach not only has an improved search ability but also allows for a flexible score function under the acyclicity constraint.

1 Introduction

Discovering and understanding causal mechanisms underlying natural phenomena are important to many disciplines of sciences. An effective approach is to conduct controlled randomized experiments, which however is expensive or even impossible in certain fields such as social sciences (Bollen, 1989) and bioinformatics (Opgen-Rhein and Strimmer, 2007). Causal discovery methods that infer causal relationships from passively observable data are hence attractive and have been an important research topic in the past decades (Pearl, 2009; Spirtes et al., 2000; Peters et al., 2017).

A major class of such causal discovery methods are score-based, which assign a score $\mathcal{S}(\mathcal{G})$, typically computed with the observed data, to each graph $\mathcal{G}$ and then search over the space of all Directed Acyclic Graphs (DAGs) for the best scoring:

$$\min_{\mathcal{G}} \ \mathcal{S}(\mathcal{G}), \ \text{subject to} \ \mathcal{G} \in \text{DAGs.} \tag{1}$$

While there have been well-defined score functions such as the Bayesian Information Criterion (BIC) or Minimum Description Length (MDL) score (Schwarz, 1978; Chickering, 2002) and the Bayesian Gaussian equivalent (BGe) score (Geiger and Heckerman, 1994) for linear-Gaussian models, Problem (1) is generally NP-hard to solve (Chickering, 1996; Chickering et al., 2004), largely due to its combinatorial nature of the acyclicity constraint with the number of DAGs increasing super-exponentially in the number of graph nodes. To tackle this problem, most existing approaches rely on local heuristics to enforce the acyclicity. For example, Greedy Equivalence Search (GES) enforces acyclicity one edge at a time, explicitly checking for the acyclicity constraint when an edge is added. GES is known to find the global minimizer with infinite samples under suitable assumptions (Chickering, 2002; Nandy et al., 2018), but this is not guaranteed in the finite sample regime. There are also hybrid methods that use constraint-based approaches to reduce the search space before applying score-based methods, e.g., the max-min hill climbing method (Tsamardinos et al., 2006). However, this methodology lacks a principled way of choosing a problem-specific combination of score functions and search strategies.

Recently, Zheng et al. (2018) introduced a smooth characterization for the acyclicity constraint, and Problem (1) can be formulated as a continuous optimization problem w.r.t. the weighted graph adjacency matrix by picking a proper loss function, e.g., the least squares loss. Subsequent works Yu et al. (2019) and Lachapelle et al. (2019) have also adopted the evidence lower bound and the negative log-likelihood as loss functions, and used Neural Networks (NNs) to model the causal relationships. Note that the loss functions in these methods must be carefully chosen in order to apply continuous optimization methods. However, many effective score functions, e.g., the generalized score function proposed by Huang et al. (2018) and the independence based score function provided in Peters et al. (2014), either cannot be represented in closed forms or have very complicated equivalent loss functions, and thus cannot be easily combined with this approach.

We propose to use Reinforcement Learning (RL) to search for the DAG with the best score according to a predefined score function, as outlined in Figure 1. The insight is that an RL agent with stochastic policy can determine automatically where to search given the uncertainty information of the learned policy, which gets updated promptly by the stream of reward signals. To apply RL to causal discovery, we use an encoder-decoder model to generate directed graphs from the observed data, which are then used to compute rewards consisting of the predefined score function as well as two penalty terms to enforce acyclicity. We resort to the actor-critic algorithm (Konda and Tsitsiklis, 2000) and stochastic methods to train the weights of the NNs, and our output is the graph that achieves the best reward, among all graphs generated in the training process. Experiments on both synthetic and real datasets show that our approach has a much improved search ability without sacrificing any flexibility in choosing score functions. In particular, the proposed approach using BIC as score function outperforms GES with the same score function on linear non-Gaussian acyclic model (LiNGAM) and linear-Gaussian datasets, and also outperforms recent gradient based methods when the causal relationships are nonlinear. Codes and datasets used in this work will be released at a later time.
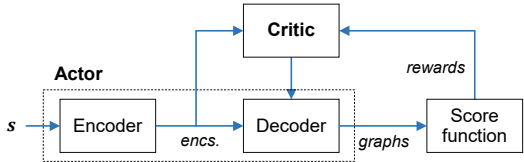

Figure 1: Reinforcement learning for score-based causal discovery.

2 RELATED WORK

Constraint-based methods first use conditional independence tests to find causal skeleton and then determine the orientations of the edges up to the Markov equivalence class, which usually contains DAGs that can be structurally diverse and may still have many unoriented edges. Examples include Sun et al. (2007); Zhang et al. (2012) that use kernel-based conditional independence criteria and the well-known PC algorithm (Spirtes et al., 2000). This class of methods involve a multiple testing problem where the tests are usually conducted independently. The testing results may have conflicts and handling them is not easy, though there are certain works, e.g., Hyttinen et al. (2014), attempting to tackle this problem. These methods are also not robust as small errors in building the graph skeleton can result in large errors in the inferred Markov equivalence class.

Another class of causal discovery methods are based on properly defined functional causal models. Unlike constraint-based methods that assume faithfulness and identify only the Markov equivalence class, these methods are able to distinguish between different DAGs in the same equivalence class, thanks to the additional assumptions on data distribution and/or functional classes. Examples include LiNGAM (Shimizu et al., 2006; 2011), the nonlinear additive noise model (Hoyer et al., 2009; Peters et al., 2014; 2017), and the post-nonlinear causal model (Zhang and Hyvärinen, 2009).

Besides Yu et al. (2019); Lachapelle et al. (2019), other recent NN based approaches to causal discovery include Goudet et al. (2018) that proposes causal generative NNs to functional causal modeling with a prior knowledge of initial skeleton of the causal graph and Kalainathan et al. (2018) that learns causal generative models in an adversarial way but does not guarantee acyclicity.

Recent advances in sequence-to-sequence learning (Sutskever et al., 2014) have motivated the use of NNs for optimization in various domains (Vinyals et al., 2015; Zoph and Le, 2017; Chen et al., 2017). A particular example is the traveling salesman problem (TSP) which was revisited in the work of pointer networks (Vinyals et al., 2015). Authors proposed a recurrent neural network with nonparametric softmaxes trained in a supervised manner to predict the sequence of visited cities. Realizing that getting high-quality labeled data is expensive and may be infeasible for new problems, Bello et al. (2016) proposed to use the RL paradigm to tackle the combinatorial problems due to their relatively simple reward mechanisms. It was shown that an RL agent can have a better generalization even when the optimal solutions are used as labeled data in the previous supervised approach.

Besides Bello et al. (2016), there are many other successful RL applications in recent years, e.g., AlphaGo (Silver et al., 2017), where the typical goal is to learn a policy for certain tasks. An exception is the work of Zoph and Le (2017) which used RL to search for neural architectures. While we use a similar idea as the RL paradigm can naturally include the search task, our work is different in the actor and reward designs: our actor is an encoder-decoder model that generates graph adjacency matrices (cf. Section 4) and the reward is tailored for causal discovery by incorporating both a score function and the acyclicity constraint (cf. Section 5.1).

3 MODEL DEFINITION

We assume the following model for data generating procedure, as in Hoyer et al. (2009); Peters et al. (2014). Each variable x_i is associated with a node i in a d-node DAG $\mathcal{G}$, and the observed value of x_i is obtained as a function of its parents in the graph plus an independent additive noise n_i, i.e.,

$$x_i := f_i(\mathbf{x}_{\mathrm{pa}(i)}) + n_i, i = 1, 2, \cdots, d,$$

where $\mathbf{x}_{\mathrm{pa}(i)}$ denotes the set of variables x_j so that there is an edge from x_j to x_i in the graph, and the noises n_i are assumed to be jointly independent. We also assume causal minimality, which in this case reduces to that each function f_i is not a constant in any of its arguments (Peters et al., 2014). We do not restrict specific forms for the functions f_i and noises n_i, but such information can be beneficial to infer causal relationships. If all the functions f_i are linear and the noises n_i are Gaussian distributed, this model yields the class of standard linear-Gaussian model that has been studied in Spirtes et al. (2000); Geiger and Heckerman (1994); Bollen (1989); Peters et al. (2017). When the functions are linear but the noises are non-Gaussian, one can obtain the LiNGAM described in Shimizu et al. (2006; 2011) and the true DAG can be uniquely identified under favorable conditions.

In this paper, we consider that all the variables x_i are scalars; extending to more complex cases is straightforward with a properly defined score function. The observed data $\mathbf{X}$, consisting of a number of vectors $\mathbf{x} := [x_1, x_2, \cdots, x_d]^T \in \mathbb{R}^d$, are then sampled independently according to the above model on an unknown DAG, with fixed functions f_i and fixed distributions for n_i. The objective of causal discovery is to use the observed data $\mathbf{X}$, which gives the empirical version of the joint distribution of $\mathbf{x}$, to infer the underlying causal DAG $\mathcal{G}$.

4 NEURAL NETWORK ARCHITECTURE FOR GRAPH GENERATION

Given a dataset $\mathbf{X} = \{\mathbf{x}^k\}_{k=1}^D$ where $\mathbf{x}^k$ denotes the k-th observed sample, we want to infer the causal graph that best describes the data generating procedure. We would like to use NNs to infer the causal graph from the observed data; specifically, we aim to design an NN based graph generator whose input is the observed data and the output is a graph adjacency matrix. A naive approach would be to use a feed-forward NN to output d^2 scalars and then reshape them to an adjacency matrix lying in $\mathbb{R}^{d \times d}$. However, this NN structure failed to produce promising results, possibly because the feed-forward NNs could not provide sufficient interactions amongst variables to capture the causal relationships from the observed data.

Motivated by recent advances in neural combinatorial optimization, particularly the pointer networks (Bello et al., 2016; Vinyals et al., 2015), we draw n random samples (with replacement) $\{\mathbf{x}^l\}$ from $\mathbf{X}$ and reshape them as $\mathbf{s} := \{\tilde{\mathbf{x}}_i\}_{i=1}^d$ where $\tilde{\mathbf{x}}_i \in \mathbb{R}^n$ is the vector concatenating all the i-th entries of the vectors in $\{\mathbf{x}^l\}$. In an analogy to the TSP problem, this represents a sequence of d cities lying in an n-dim space. We are concerned with generating a binary adjacency matrix $A \in \{0, 1\}^{d \times d}$ such

that the corresponding graph is a DAG and achieves the best score. In this work, we consider existing encoder-decoder models for graph generation:

Encoder   We use the attention based encoder in the Transformer structure proposed by Vaswani et al. (2017). We believe that the self-attention scheme is capable of finding the causal relationships amongst variables. Other attention based models such as graph attention network (Veličković et al., 2018) may also be used, which will be considered in a future work. Denote the output of the encoder by enc_i with dimension d_e, corresponding to each input $\tilde{\mathbf{x}}_i$.

Decoder   Our decoder generates the graph adjacency matrix in an element-wise manner, by building relationships between two encoder outputs. We consider the single layer decoder

$$g_{ij}(W_1, W_2, u) = u^T \tanh(W_1 enc_i + W_2 enc_j),$$

where $W_1, W_2 \in \mathbb{R}^{d_h \times d_e}$, $u \in \mathbb{R}^{d_h \times 1}$ are trainable parameters and d_h is the hidden dimension associated with the decoder. To generate a binary adjacency matrix A, we pass each entry g_{ij} into a logistic sigmoid function $\sigma(\cdot)$ and then sample according to a Bernoulli distribution with probability $\sigma(g_{ij})$, which indicates the probability of existing an edge from x_i to x_j. To avoid self-loop, we simply mask the (i,i)-th entry in the adjacency matrix.

It is also possible to use the neural tensor network model from Socher et al. (2013) and the bilinear model to build the pairwise relationships between encoder outputs. Another choice is the Transformer structure which generates an adjacency matrix in a row-wise manner. Empirically, we find that the single layer decoder performs the best, possibly because it contains less parameters and is easier to train to find better DAGs, while the attention based Transformer encoder has provided sufficient interactions amongst the variables for causal discovery. In Appendix A, we give more details on the above decoders and their empirical results with linear-Gaussian datasets.

5   REINFORCEMENT LEARNING FOR SEARCH

In this section, we propose to use RL as the search strategy for finding the DAG with the best score, outlined in Figure 1. As one will see, the proposed method improves the search ability over traditional score-based methods and also allows for flexible score functions under the acyclicity constraint.

5.1   SCORE FUNCTION, ACYCLICITY, AND REWARD

Score Function   In this work, we consider only existing score functions to construct the reward that will be maximized by an RL agent. Often score-based methods assume a parametric model for causal relationships (e.g., linear-Gaussian equations or multinomial distributions), which introduces a set of parameters θ. Among all score functions that can be directly included here, we focus on the BIC score which has been shown to be not only consistent (Haughton et al., 1988) but also locally consistent for its decomposability (Chickering, 1996).

The BIC score for a given directed graph $\mathcal{G}$ is

$$\mathcal{S}_{\text{BIC}}(\mathcal{G}) = -2\log p(\mathbf{X}; \hat{\theta}, \mathcal{G}) + d_\theta \log n,$$

where $\hat{\theta}$ is the maximum likelihood estimator and d_θ denotes the dimensionality of the parameter θ. We assume i.i.d. Gaussian additive noises throughout this paper. If we apply linear models to each causal relationship and let $\hat{x}_i^k$ be the corresponding estimate for x_i^k, the i-th entry in the k-th observed sample, then we have the BIC score being (up to some additive constant)

$$\mathcal{S}_{\text{BIC}}(\mathcal{G}) = \sum_{i=1}^{d} \left(n\log(\text{RSS}_i/n) \right) + \#(\text{edges})\log n, \tag{2}$$

where $\text{RSS}_i = \sum_{k=1}^{D}(x_i^k - \hat{x}_i^k)^2$ denotes the residual sum of squares. The first term in Eq. (2) is equivalent to the log-likelihood objective used by GraN-DAG (Lachapelle et al., 2019) and the second term adds penalty on the number of edges in the graph $\mathcal{G}$. Further assuming that the noise variances are equal (despite the fact that they may be different), we have

$$\mathcal{S}_{\text{BIC}}(\mathcal{G}) = nd\log\left(\left(\sum_{i=1}^{d} \text{RSS}_i \right) /(nd) \right) + \#(\text{edges})\log n. \tag{3}$$

We notice that $\sum_i \mathrm{RSS}_i$ is the least squares loss used in NOTEARS (Zheng et al., 2018). Besides assuming linear models, other regression methods like Gaussian process regression (GPR) can also be used to estimate x_i^k. In Section 6, we will use quadratic regression and GPR to model causal relationships with the observed data for our experiments.

Acyclicity   A remaining issue is the acyclicity constraint. Other than GES that explicitly checks for acyclicity each time an edge is added, we add penalty terms w.r.t. acyclicity to the score function to enforce acyclicity in an implicit way and allow the generated graph to change more than one edges at each iteration. Among all the functions that compute some 'distance' from a directed graph to DAGs, e.g., the total length along all cyclic paths of the graph, we use a recent result from Zheng et al. (2018): a directed graph $\mathcal{G}$ with binary adjacency matrix A is acyclic if and only if

$$h(A) := \mathrm{trace}\left(e^A\right) - d = 0, \tag{4}$$

where e^A is the matrix exponential of A. We find that $h(A)$, which is non-negative, can be small for certain cyclic graphs and its minimum over all non-DAGs is not easy to compute. Consequently, we would require a very large penalty weight to obtain exact DAGs if only $h(A)$ is used. As such, we add another penalty term, the indicator function w.r.t. acyclicity, to induce exact DAGs.

Reward   Our final reward incorporates both the score function and the acyclicity constraint:

$$\mathrm{reward} := -\left[\mathcal{S}(\mathcal{G}) + \lambda_1 \mathbf{I}(\mathcal{G} \notin \mathsf{DAGs}) + \lambda_2 h(A)\right], \tag{5}$$

where $\mathbf{I}(\cdot)$ denotes the indicator function and $\lambda_1, \lambda_2 \geq 0$ are two penalty parameters. It is not hard to see that the larger λ_1 and λ_2 are, the more likely a generated graph with a high reward is acyclic. We then aim to maximize the reward over all possible directed graphs, or equivalently, we have

$$\min_{\mathcal{G}} \ \left[\mathcal{S}(\mathcal{G}) + \lambda_1 \mathbf{I}(\mathcal{G} \notin \mathsf{DAGs}) + \lambda_2 h(A)\right]. \tag{6}$$

An interesting question is whether this new formulation is equivalent to the original problem with hard acyclicity constraint. Fortunately, the following proposition guarantees that Problems (1) and (6) are equivalent with properly chosen λ_1 and λ_2, which can be verified by showing that a minimizer of one problem is also a solution to the other. A proof is provided in Appendix B for completeness.

Proposition 1. *Let $h_{\min} > 0$ be the minimum of $h(A)$ over all directed cyclic graphs, i.e., $h_{\min} = \min_{\mathcal{G} \notin \mathsf{DAGs}} h(A)$. Let $\mathcal{S}^*$ denote the optimal score achieved by some DAG in Problem (1). Assume that $\mathcal{S}_L \in \mathbb{R}$ is a lower bound of the score function over all possible directed graphs, i.e., $S_L \leq \min_{\mathcal{G}} \mathcal{S}(\mathcal{G})$, and $S_U \in \mathbb{R}$ is an upper bound on the optimal score with $\mathcal{S}^* \leq \mathcal{S}_U$. Then Problems (1) and (6) are equivalent if*

$$\lambda_1 + \lambda_2 h_{\min} \geq \mathcal{S}_U - \mathcal{S}_L.$$

For practical use, we need to find respective quantities in order to choose proper penalty parameters. An upper bound $\mathcal{S}_U$ can be easily found by drawing some random DAGs or using the resulting DAGs from existing methods like NOTEARS. A lower bound $\mathcal{S}_L$ may depend on the particular score function. With BIC score, we can fit each variable x_i against all the rest variables, and use only the RSS_i terms but ignore the additive penalty term on the number of edges. With the independence based score function proposed by Peters et al. (2014), we may simply set $\mathcal{S}_L = 0$. The minimum term $h_{\min}$, as previously mentioned, may be not easy to find. Fortunately, with $\lambda_1 = \mathcal{S}_U - \mathcal{S}_L$, Proposition 1 guarantees the equivalence of Problems (1) and (6) for any $\lambda_2 \geq 0$. We will pick a relatively small value for λ_2, which helps to generate directed graphs that become closer to DAGs.

Empirically, we find that if the penalty weights are set too large, the score function would have little effect on the reward and the RL agent usually finds DAGs with high scores. Similar to Lagrangian methods, we will start with small penalty weights and gradually increase them so that the condition in Proposition 1 is satisfied. Meanwhile, we notice that the second penalty term $h(A)$ is independent of the particular range of score functions, so we also adjust the predefined scores to a certain range, e.g., $[0, \mathcal{S}_0]$ by using $\mathcal{S}_0(\mathcal{S} - \mathcal{S}_L)/(\mathcal{S}_U - \mathcal{S}_L)$ for some $\mathcal{S}_0 > 0$. Our algorithm is summarized in Algorithm 1. In all our experiments, $\mathcal{S}_L$ is obtained from a complete directed graph and $\mathcal{S}_U$ is from an empty graph. Since $\mathcal{S}_U$ with the empty graph can be very high for large graphs, we also update it by keeping track of the lowest score achieved by DAGs generated during training. Other parameter choices are $\mathcal{S}_0 = 5$, $t_0 = 1000$, $\lambda_1 = 0$, $\Delta_1 = 1$, $\lambda_2 = \lceil d/3 \rceil$, and $\Delta_2 = 10$. The weight λ_2 is updated in a similar manner to the updating rule on the Lagrangian multiplier used by NOTEARS and we pick $\Lambda_2 = 0.01$ as an upper bound on λ_2, as previously discussed.

Algorithm 1 The proposed RL approach for score-based causal discovery

---

Require: score parameters: $\mathcal{S}_L$, $\mathcal{S}_U$, and $\mathcal{S}_0$; penalty parameters: λ_1, Δ_1, λ_2, Δ_2, and Λ_2; iteration number for parameter update: t_0.

1: **for** $t = 1, 2, \ldots$ **do**
2:     Run actor-critic algorithm, with score adjustment by $\mathcal{S} \leftarrow \mathcal{S}_0(\mathcal{S} - \mathcal{S}_L)/(\mathcal{S}_U - \mathcal{S}_L)$
3:     **if** $t \pmod{t_0} = 0$ **then**
4:         **if** the maximum reward corresponds to a DAG with score $\mathcal{S}_{\min}$ **then**
5:             update $\mathcal{S}_U \leftarrow \mathcal{S}_{\min}$
6:         update $\lambda_1 \leftarrow \min(\lambda_1 + \Delta_1, \mathcal{S}_U)$ and $\lambda_2 \leftarrow \min(\lambda_2\Delta_2, \Lambda_2)$.
7:         update recorded rewards according to new λ_1 and λ_2

5.2 ACTOR-CRITIC ALGORITHM

We believe that the exploitation and exploration scheme in the RL paradigm provide an appropriate way to guide the search. Let ψ denote the parameters of the NNs for graph generation. Our training objective is the expected reward defined as

$$J(\psi \mid \mathbf{s}) = \mathbb{E}_{A \sim \pi(\cdot \mid \mathbf{s})} \left\{ - \left[\mathcal{S}(\mathcal{G}) + \lambda_1 \mathbf{I}(\mathcal{G} \notin \mathsf{DAGs}) + \lambda_2 h(A) \right] \right\}. \tag{7}$$

During training, the input $\mathbf{s}$ is constructed by randomly drawing samples from the observed dataset $\mathbf{X}$, as described in Section 4.

We resort to policy gradient methods and stochastic methods to optimize the parameters ψ. The gradient of Eq. (7) can be obtained by the well-known REINFORCE algorithm (Williams, 1992; Sutton et al., 2000). We draw B samples $\mathbf{s}_1, \mathbf{s}_2, \ldots, \mathbf{s}_B$ as a batch to estimate the gradient which is then used to train the NNs through stochastic optimization methods like Adam (Kingma and Ba, 2014). Using a parametric baseline to estimate the reward can also help training (Konda and Tsitsiklis, 2000). For the present work, our critic is a simple 2-layer feed-forward NN with ReLU units, with the input being the encoder outputs $\{enc_i\}$. The critic is trained with Adam on a mean squared error between its predictions and the true rewards. An entropy regularization term (Williams and Peng, 1991; Mnih et al., 2016) is also added to encourage exploration of the RL agent. Although policy gradient methods only guarantee local convergence (Sutton et al., 2000), here we remark that the inferred graphs from the actor-critic algorithm are all DAGs in our experiments.

Training an RL agent typically requires many iterations. In the present work, we find that computing the rewards for generated graphs is much more time-consuming than training NNs. Therefore, we record the computed rewards corresponding to different graph structures. Moreover, the BIC score can be decomposed according to single causal relationships and we also record the corresponding RSS_i to avoid repeated computations.

5.3 FINAL OUTPUT

Since we are concerned with finding a DAG with the best score rather than a policy, we record all the graphs generated during the training process and output the one with the best reward. In practice, the graph may contain spurious edges and further processing is needed.

To this end, we can prune the estimated edges in a greedy way, according to either the regression performance or the score function. For an inferred causal relationship, we remove a parental variable and calculate the performance of the resulting graph, with all other causal relationships unchanged. If the performance does not degrade or degrade within a predefined tolerance, we accept pruning and continue this process with the pruned causal relationship. For linear models, pruning can be simply done by thresholding the estimated coefficients. Besides, we observe that the top few graphs, ranked by their rewards, are usually structurally similar. Thus, we can conduct a majority vote to select common edges in these graphs that are potentially more important to achieving high rewards. Notice that a majority vote might result in a cyclic graph. In this case, we can apply previous pruning strategy with a decreasing tolerance or an increasing threshold until a DAG is obtained.

Related to the above pruning process is to add to the reward an increased penalty weight on the number of edges of a given graph. However, this weight is not easy to choose, as a large weight may incur missing edges. In this work, we stick to the penalty weight $\log n$ that is included in the BIC score and then apply pruning to the inferred graph in order to remove spurious edges.

6 EXPERIMENTAL RESULTS

We report empirical results on synthetic and real datasets to compare our approach against both traditional and recent gradient based approaches, including GES (with BIC score) (Chickering, 2002; Ramsey et al., 2017), the PC algorithm (with Fisher-z test and p-value 0.01) (Spirtes et al., 2000), ICA-LiNGAM (Shimizu et al., 2006), the Causal Additive Model (CAM) based algorithm proposed by Bühlmann et al. (2014), NOTEARS (Zheng et al., 2018), DAG-GNN (Yu et al., 2019), and GraN-DAG (Lachapelle et al., 2019), among others. All these algorithms have available implementations and we give a brief description on these algorithms and their implementations in Appendix C. Default hyper-parameters of these implementations are used unless otherwise stated. For pruning, we use the same thresholding method for ICA-LiNGAM, NOTEARS, and DAG-GNN. Since the authors of CAM and GraN-DAG proposed to apply significance testing of covariates based on generalized additive models and then declare significance if the reported p-values are lower than or equal to 0.001, we stick to the same pruning method for CAM and GraN-DAG.

The proposed RL based approach is implemented based on an existing Tensorflow (Abadi et al., 2016) implementation of neural combinatorial optimizer (see Appendix C for more details). The decoder is modified as described in Section 4 and the RL algorithm related hyper-parameters are left unchanged. We pick $B = 64$ as batch size at each iteration and $d_h = 16$ as the hidden dimension with the single layer decoder. Our approach is combined with the BIC scores under Gaussianity assumption given in Eqs. (2) and (3), and are denoted as RL-BIC and RL-BIC2, respectively.

We evaluate the estimated graphs using three metrics: False Discovery Rate (FDR), True Positive Rate (TPR), and Structural Hamming Distance (SHD) which is the smallest number of edge additions, deletions, and reversals to convert the estimated graph into the true DAG. Since GES and PC may output unoriented edges, we follow Zheng et al. (2018) to treat GES favorably by regarding undirected edges as true positives as long as the true graph has a directed edge in place of the undirected edge.

6.1 LINEAR MODEL WITH GAUSSIAN AND NON-GAUSSIAN NOISE

Given number of variables d, we generate a $d \times d$ upper triangular matrix as the graph binary adjacency matrix, in which the upper entries are sampled independently from $\text{Bern}(0.5)$. We assign edge weights independently from $\text{Unif}([-2, -0.5] \cup [0.5, 2])$ to obtain a weight matrix $W \in \mathbb{R}^{d \times d}$, and then sample $\mathbf{x} = W^T \mathbf{x} + \mathbf{n} \in \mathbb{R}^d$ from both Gaussian and non-Gaussian noise models. The non-Gaussian noise is the same as the one used for ICA-LiNGAM (Shimizu et al., 2006), which generates samples from a Gaussian distribution and passes them through a power nonlinearity to make them non-Gaussian. We pick unit variances for all noises in both models and generate $D = 5,000$ samples as our datasets. A random permutation of variables is then performed. This data generating procedure is similar to that used by NOTEARS and DAG-GNN and the true causal graphs in both cases are known to be identifiable (Peters and Bühlmann, 2013; Shimizu et al., 2006).

We first consider graphs with $d = 12$ nodes. We use $n = 64$ for constructing the input sample and set the maximum number of iterations to $20,000$. Figure 2 shows the learning process of the proposed method RL-BIC2 on a linear-Gaussian dataset. We use a threshold 0.3, same as NOTEARS and DAG-GNN with this data model, to prune the estimated edges. In this example, RL-BIC2 generates $683,784$ different graphs during training, much lower than the total number (around 5.22×10^{26}) of DAGs. The pruned DAG turns out to be exactly the same as the underlying causal graph.

We report the empirical results on LiNGAM and linear-Gaussian data models in Table 1. Both PC and GES perform poorly, possibly because we consider relatively dense graphs for our data generating procedure. CAM does not perform well either, as it assumes nonlinear causal relationships. ICA-LiNGAM recovers all the true causal graphs for LiNGAM data but performs poorly on linear-Gaussian data. This is not surprising because ICA-LiNGAM works for non-Gaussian noise and does not provide guarantee for linear-Gaussian datasets. We see that both NOTEARS and DAG-GNN have good causal discovery results whereas GraN-DAG performs much worse. We believe that it is because GraN-DAG uses 2-layer feed-forward NNs to model the causal relationships, which can hardly learn a good linear relationship. Modifying the feed-forward NNs to linear functions then reduces to NOTEARS with negative log-likelihood as loss function, which yields similar performance on these datasets (see Appendix D.1 for detailed results). As to our proposed methods, we observe that RL-BIC2 recovers all the true causal graphs on both data models in this experiment while
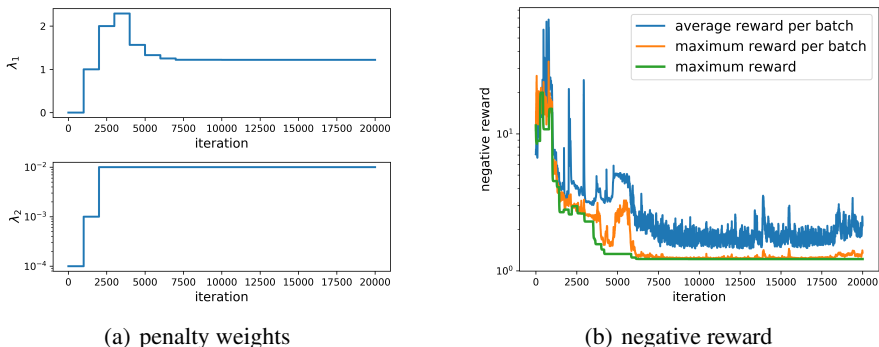
(a) penalty weights

(b) negative reward

Figure 2: Learning process of the proposed method RL-BIC2 on a Linear-Gaussian dataset.

Table 1: Empirical results on LiNGAM and linear-Gaussian data models with 12-node graphs

		RL-BIC	RL-BIC2	PC	GES	ICA-LiNGAM	CAM	NOTEARS	DAG-GNN	GraN-DAG
LiNGAM	FDR	0.28 ± 0.11	0 ± 0	0.06 ± 0.04	0.62 ± 0.06	0 ± 0	0.67 ± 0.08	0.04 ± 0.03	0.11 ± 0.03	0.63 ± 0.10
	TPR	0.71 ± 0.17	1 ± 0	0.25 ± 0.03	0.25 ± 0.04	1 ± 0	0.49 ± 0.07	0.95 ± 0.05	0.94 ± 0.04	0.37 ± 0.15
	SHD	17.4 ± 7.50	0 ± 0	31.8 ± 2.04	32.8 ± 2.93	0 ± 0	40.4 ± 5.92	2.40 ± 2.42	5.00 ± 1.41	36.0 ± 5.33
Linear-Gaussian	FDR	0.38 ± 0.13	0 ± 0	0.52 ± 0.07	0.63 ± 0.06	0.65 ± 0.02	0.70 ± 0.08	0.02 ± 0.02	0.10 ± 0.05	0.70 ± 0.17
	TPR	0.66 ± 0.12	1 ± 0	0.31 ± 0.03	0.24 ± 0.04	0.73 ± 0.05	0.44 ± 0.11	0.98 ± 0.02	0.95 ± 0.05	0.27 ± 0.13
	SHD	22.2 ± 6.34	0 ± 0	29.6 ± 3.01	33.2 ± 2.48	46.2 ± 2.79	40.8 ± 4.53	1.00 ± 0.89	4.40 ± 2.06	38.2 ± 6.68

RL-BIC has a worse performance. One may wonder whether this observation is due to the same noise variances that are used in our data models; we conduct additional experiments where the noise variances are randomly sampled and RL-BIC2 still outperforms RL-BIC by a large margin (see also Appendix D.1). Nevertheless, with the same BIC score, RL-BIC2 performs much better than GES on both datasets, indicating that the RL approach brings in a greatly improved search ability.

Finally, we test the proposed method on larger graphs with $d = 30$ nodes, where the upper entries are sampled independently from $\mathrm{Bern}(0.2)$. This edge probability choice corresponds to graphs with average degree 3 considered in Yu et al. (2019). This setting becomes more difficult due to the significantly increased search space. We choose a larger number of observed samples, $n = 128$, to construct the input for graph generator and increase the training iterations to $35,000$. On LiNGAM datasets, RL-BIC2 has FDR, TPR, and SHD being 0.18 ± 0.08, 0.87 ± 0.05, and 27.23 ± 13.16, respectively. There is one dataset with which RL-BIC2 performed very poorly. Removing this dataset, RL-BIC2 has an average SHD 20, slightly worse than NOTEARS with an average SHD 17.2.

6.2 NONLINEAR MODELS WITH QUADRATIC FUNCTIONS

We now consider nonlinear causal relationships with quadratic functions. We generate an upper triangular matrix in a similar way to the first experiment. For a causal relationship with parents $\mathbf{x}_{\mathrm{pa}(i)} = [x_{i_1}, x_{i_2}, \ldots]^T$ at the i-th node, we expand $\mathbf{x}_{\mathrm{pa}(i)}$ to contain both first- and second-order features. The coefficient for each term is then either 0 or sampled from $\mathrm{Unif}\,([-2, -0.5] \cup [0.5, 2])$, with equal probability. If a parent variable does not appear in any feature term with a non-zero coefficient, then we remove the corresponding edge in the causal graph. The rest follows the same as in first experiment and here we use the non-Gaussian noise model with $5,000$ samples. The true causal graph is identifiable according to Peters et al. (2014). For this quadratic model, there may exist very large variable values which cause computation issues for quadratic regression. We treat these samples as outliers and detailed processing is given in Appendix D.2.

We use quadratic regression for a given causal relationship and calculate the BIC score (assuming equal noise variances) in Eq. (3). For pruning, we simply apply thresholding, with threshold as 0.3, to the estimated coefficients of both first- and second-order terms. If the coefficient of a second-order term, e.g., $x_{i_1} x_{i_2}$, is non-zero after thresholding, then we have two directed edges that are from x_{i_1} to x_i and from x_{i_2} to x_i, respectively. We do not consider PC and GES in this experiment due to their

Table 2: Empirical results on nonlinear models with quadratic functions

	RL-BIC2	NOTEARS	NOTEARS-2	NOTEARS-3	ICA-LiNGAM	CAM	DAG-GNN	GraN-DAG
FDR	0.02 ± 0.04	0.35 ± 0.06	0.15 ± 0.10	0 ± 0	0.47 ± 0.06	0.32 ± 0.17	0.39 ± 0.04	0.40 ± 0.17
TPR	0.98 ± 0.04	0.71 ± 0.16	0.70 ± 0.15	0.79 ± 0.20	0.76 ± 0.09	0.78 ± 0.05	0.55 ± 0.14	0.73 ± 0.16
SHD	0.60 ± 1.20	14.8 ± 3.37	8.80 ± 3.82	5.20 ± 5.19	20.4 ± 5.00	14.1 ± 5.12	18.0 ± 2.45	39.6 ± 5.85

poor performance in the first experiment. Our results with 10-node graphs are reported in Table 2, which shows that RL-BIC2 achieves the best performance.

For fair comparison, we apply the same quadratic regression based pruning method to the outputs of NOTEARS, denoted as NOTEARS-2. We see that this pruning further reduces FDR, i.e., removes spurious edges, with little effect on TPR. Since pruning does not help discover additional positive edges or increase TPR, we will not apply this pruning method to other methods as their TPRs are much lower than that of RL-BIC2. Finally, with prior knowledge that the function form is quadratic, we can modify NOTEARS to apply quadratic functions to modeling the causal relationships, with an equivalent weighted adjacency matrix constructed using the coefficients of the first- and second-order terms, similar to the idea used by GraN-DAG (detailed derivations are given in Appendix D.2). The problem then becomes a nonconvex optimization problem with $(d - 1)d^2/2$ parameters (which are the coefficients of both first- and second-order features), compared to the original problem with d^2 parameters. This method corresponds to NOTEARS-3 in Table 2. Despite the fact that NOTEARS-3 did not achieve a better overall performance than RL-BIC2, we comment that it discovered almost correct causal graphs (with SHD ≤ 3) on more than half of the datasets, but performed poorly on the rest datasets. We believe that it is due to the increased number of optimization parameters which makes the optimization problem harder to solve. Meanwhile, we do not exclude that NOTEARS-3 can achieve a better causal discovery performance with other optimization methods.

6.3 NONLINEAR MODELS WITH GAUSSIAN PROCESSES

Given a randomly generated causal graph, we consider another nonlinear model where each causal relationship f_i is a function sampled from a Gaussian process, with RBF kernel of bandwidth one. The additive noise n_i is normally distributed with variance sampled uniformly. This setting is known to be identifiable according to Peters et al. (2014). We use a setup that is also considered by GraN-DAG (Lachapelle et al., 2019): 10-node and 40-edge graphs with 1000 generated samples. The empirical results are reported in Table 3.

Table 3: Empirical results on nonlinear models with Gaussian processes

	RL-BIC	RL-BIC2	ICA-LiNGAM	NOTEARS	DAG-GNN	GraN-DAG	CAM
FDR	0.14 ± 0.03	0.17 ± 0.15	0.48 ± 0.04	0.48 ± 0.19	0.36 ± 0.11	0.12 ± 0.08	0.15 ± 0.07
TPR	0.96 ± 0.03	0.80 ± 0.09	0.63 ± 0.07	0.18 ± 0.09	0.07 ± 0.03	0.81 ± 0.05	0.82 ± 0.04
SHD	6.20 ± 1.33	13.8 ± 2.56	48.4 ± 6.56	12.0 ± 5.18	34.6 ± 1.36	10.2 ± 2.39	10.2 ± 2.93

One can see that ICA-LiNGAM, NOTEARS, and DAG-GNN perform poorly on this data model. A possible reason is that they may not be able to model this type of causal relationship. More importantly, these methods operate on the weighted adjacency matrix which is not obvious with here. For our method, we apply Gaussian process regression (GPR) with RBF kernel to model the causal relationships. Notice that even though the observed data are from a function sampled from Gaussian process, it is not guaranteed that GPR with the same kernel of bandwidth one can achieve a good performance. Indeed, using a fixed kernel bandwidth would lead to severe overfitting that incurs many spurious edges and the graph with the highest reward is usually not a DAG. To proceed, we normalize the observed data and apply median heuristics for kernel bandwidth. Both our methods perform reasonably well, with RL-BIC outperforming all the other methods.

We also use majority vote as a way of pruning spurious edges, which lead to almost the same results as reported in the table. The minor difference seems to indicate that the penalty weight $\log n$ on the number of edges is good enough to remove spurious edges for this experiment. We also check the results of GraN-DAG and CAM before applying CAM pruning. We have (FDR, TPR, SHD)

$0.17 \pm 0.07, 0.89 \pm 0.03, 8.60 \pm 3.01$ and $0.18 \pm 0.07, 0.92 \pm 0.05, 8.00 \pm 3.10$ for GraN-DAG and CAM, respectively, showing that CAM pruning removes more true edges with this dataset.

6.4 REAL DATA

We consider a real dataset to discover a protein signaling network based on expression levels of proteins and phospholipids (Sachs et al., 2005). This dataset is a common benchmark in graphical models, with experimental annotations well accepted by the biological community. Both observational and interventional data are contained in this dataset. Since we are interested in using observational data to infer causal mechanisms, we only consider the observational data with $n = 853$ samples. The ground truth causal graph given by Sachs et al. (2005) has 11 nodes and 17 edges.

Notice that the true graph is indeed sparse and an empty graph can have an SHD as low as 17. Therefore, we report more detailed results regarding the estimated graph: number of total edges, number of correct edges, and the SHD. Previous works have shown PC and GES were outperformed by GraN-DAG and CAM, and we will not report the results from PC and GES. We apply GPR with RBF kernel to modeling the causal relationships, with the same data normalization and median heuristics for kernel bandwidth as in Section 6.3. We also use CAM pruning on the inferred graph from the training process. The empirical results are given in Table 4. Both RL-BIC and RL-BIC2 achieve promising results, compared to other methods.

Table 4: Empirical results on Sachs dataset

	RL-BIC	RL-BIC2	ICA-LiNGAM	CAM	NOTEARS	DAG-GNN	GraN-DAG
Correct Edges	6	7	4	6	6	6	5
Total Edges	10	10	8	10	20	15	10
SHD	12	11	14	12	19	16	13

7 CONCLUSION AND FUTURE WORKS

We have proposed to use RL to search for the DAG with the optimal score. Our reward is designed to incorporate a predefined score function and two penalty terms to enforce acyclicity. We use the actor-critic algorithm as our RL algorithm, where the actor is constructed based on recent encoder-decoder models. Experiments are conducted on both synthetic and real datasets to show the advantages of our method over other causal discovery methods.

We have shown the effectiveness of the proposed method with 30-node graphs, yet dealing with large graphs (with more than 50 nodes) is still challenging. Nevertheless, many real applications, like Sachs dataset Sachs et al. (2005), have a relatively small number of variables. On the other hand, it is possible to decompose large causal discovery problems into smaller ones; see, e.g., Ma et al. (2008). Prior knowledge or constraint-based methods may also be used to reduce the search space.

There are several future directions from the present work. With current implementations, computing score functions is more time consuming than training NNs. While more computing resources can definitely help accelerate training, we believe that developing an efficient and effective score function is also key to the proposed approach. Besides, there are other RL algorithms that may be used to improve the current RL algorithm. For example, the asynchronous advantage actor-critic algorithm has been shown to be effective in many applications (Mnih et al., 2016; Zoph and Le, 2017). This will be considered in a future work.

REFERENCES

M. Abadi, P. Barham, J. Chen, Z. Chen, A. Davis, J. Dean, M. Devin, S. Ghemawat, G. Irving, M. Isard, et al. Tensorflow: A system for large-scale machine learning. In *12th USENIX Symposium on Operating Systems Design and Implementation (OSDI)*, 2016.

I. Bello, H. Pham, Q. V. Le, M. Norouzi, and S. Bengio. Neural combinatorial optimization with reinforcement learning. *arXiv preprint arXiv:1611.09940*, 2016.

K. A. Bollen. *Structural Equations with Latent Variables*. Wiley, 1989.

P. Bühlmann, J. Peters, J. Ernest, et al. Cam: Causal additive models, high-dimensional order search and penalized regression. *The Annals of Statistics*, 42(6):2526–2556, 2014.

Y. Chen, M. W. Hoffman, S. G. Colmenarejo, M. Denil, T. P. Lillicrap, M. Botvinick, and N. de Freitas. Learning to learn without gradient descent by gradient descent. In *International Conference on Machine Learning*, 2017.

D. M. Chickering. Learning Bayesian networks is NP-complete. In *Learning from Data*, pages 121–130. Springer, 1996.

D. M. Chickering. Optimal structure identification with greedy search. *Journal of Machine Learning Research*, 3(Nov):507–554, 2002.

D. M. Chickering, D. Heckerman, and C. Meek. Large-sample learning of Bayesian networks is NP-hard. *Journal of Machine Learning Research*, 5(Oct):1287–1330, 2004.

D. Geiger and D. Heckerman. Learning Gaussian networks. In *Conference on Uncertainty in Artificial Intelligence*, 1994.

O. Goudet, D. Kalainathan, P. Caillou, I. Guyon, D. Lopez-Paz, and M. Sebag. Learning functional causal models with generative neural networks. In *Explainable and Interpretable Models in Computer Vision and Machine Learning*, pages 39–80. Springer, 2018.

S. W. Han, G. Chen, M.-S. Cheon, and H. Zhong. Estimation of directed acyclic graphs through two-stage adaptive LASSO for gene network inference. *Journal of the American Statistical Association*, 111(515):1004–1019, 2016.

D. M. Haughton et al. On the choice of a model to fit data from an exponential family. *The Annals of Statistics*, 16(1):342–355, 1988.

P. O. Hoyer, D. Janzing, J. M. Mooij, J. Peters, and B. Schölkopf. Nonlinear causal discovery with additive noise models. In *Advances in Neural Information Processing Systems 21*, 2009.

B. Huang, K. Zhang, Y. Lin, B. Schölkopf, and C. Glymour. Generalized score functions for causal discovery. In *Proceedings of the 24th ACM SIGKDD International Conference on Knowledge Discovery & Data Mining*, 2018.

A. Hyttinen, F. Eberhardt, and M. Järvisalo. Constraint-based causal discovery: Conflict resolution with answer set programming. In *Conference on Uncertainty in Artificial Intelligence*, 2014.

D. Kalainathan, O. Goudet, I. Guyon, D. Lopez-Paz, and M. Sebag. Structural agnostic modeling: Adversarial learning of causal graphs. *arXiv preprint arXiv:1803.04929*, 2018.

D. P. Kingma and J. Ba. Adam: A method for stochastic optimization. *ICLR*, 2014.

V. R. Konda and J. N. Tsitsiklis. Actor-critic algorithms. In *Advances in Neural Information Processing Systems*, 2000.

S. Lachapelle, P. Brouillard, T. Deleu, and S. Lacoste-Julien. Gradient-based neural dag learning. *arXiv preprint arXiv:1906.02226*, 2019.

Z. Ma, X. Xie, and Z. Geng. Structural learning of chain graphs via decomposition. *Journal of Machine Learning Research*, 9(Dec):2847–2880, 2008.

V. Mnih, A. P. Badia, M. Mirza, A. Graves, T. Lillicrap, T. Harley, D. Silver, and K. Kavukcuoglu. Asynchronous methods for deep reinforcement learning. In *ICML*, 2016.

P. Nandy, A. Hauser, M. H. Maathuis, et al. High-dimensional consistency in score-based and hybrid structure learning. *The Annals of Statistics*, 46(6A):3151–3183, 2018.

R. Opgen-Rhein and K. Strimmer. From correlation to causation networks: a simple approximate learning algorithm and its application to high-dimensional plant gene expression data. *BMC systems biology*, 1(1):37, 2007.

J. Pearl. *Causality*. Cambridge University Press, 2009.

J. Peters and P. Bühlmann. Identifiability of gaussian structural equation models with equal error variances. *Biometrika*, 101(1):219–228, 2013.

J. Peters, J. M. Mooij, D. Janzing, and B. Schölkopf. Causal discovery with continuous additive noise models. *The Journal of Machine Learning Research*, 15(1):2009–2053, 2014.

J. Peters, D. Janzing, and B. Schölkopf. *Elements of Causal Inference - Foundations and Learning Algorithms*. Adaptive Computation and Machine Learning Series. The MIT Press, Cambridge, MA, USA, 2017.

J. Ramsey, M. Glymour, R. Sanchez-Romero, and C. Glymour. A million variables and more: the fast greedy equivalence search algorithm for learning high-dimensional graphical causal models, with an application to functional magnetic resonance images. *International Journal of Data Science and Analytics*, 3(2):121–129, 2017.

K. Sachs, O. Perez, D. Pe'er, D. A. Lauffenburger, and G. P. Nolan. Causal protein-signaling networks derived from multiparameter single-cell data. *Science*, 308(5721):523–529, 2005.

G. Schwarz. Estimating the dimension of a model. *The Annals of Statistics*, 6(2):461–464, 1978.

S. Shimizu, P. O. Hoyer, A. Hyvärinen, and A. Kerminen. A linear non-Gaussian acyclic model for causal discovery. *Journal of Machine Learning Research*, 7(Oct):2003–2030, 2006.

S. Shimizu, T. Inazumi, Y. Sogawa, A. Hyvärinen, Y. Kawahara, T. Washio, P. O. Hoyer, and K. Bollen. Directlingam: A direct method for learning a linear non-Gaussian structural equation model. *Journal of Machine Learning Research*, 12(Apr):1225–1248, 2011.

D. Silver, J. Schrittwieser, K. Simonyan, I. Antonoglou, A. Huang, A. Guez, T. Hubert, L. Baker, M. Lai, A. Bolton, et al. Mastering the game of go without human knowledge. *Nature*, 550(7676): 354, 2017.

R. Socher, D. Chen, C. D. Manning, and A. Ng. Reasoning with neural tensor networks for knowledge base completion. In *Advances in Neural Information Processing Systems*, pages 926–934, 2013.

P. Spirtes, C. Glymour, and R. Scheines. *Causation, Prediction, and Search*. MIT press, Cambridge, MA, USA, 2nd edition, 2000.

X. Sun, D. Janzing, B. Schölkopf, and K. Fukumizu. A kernel-based causal learning algorithm. In *International Conference on Machine Learning*, 2007.

I. Sutskever, O. Vinyals, and Q. V. Le. Sequence to sequence learning with neural networks. In *Advances in Neural Information Processing Systems*, 2014.

R. S. Sutton, D. A. McAllester, S. P. Singh, and Y. Mansour. Policy gradient methods for reinforcement learning with function approximation. In *Advances in Neural Information Processing Systems*, 2000.

I. Tsamardinos, L. E. Brown, and C. F. Aliferis. The max-min hill-climbing bayesian network structure learning algorithm. *Machine learning*, 65(1):31–78, 2006.

A. Vaswani, N. Shazeer, N. Parmar, J. Uszkoreit, L. Jones, A. N. Gomez, Ł. Kaiser, and I. Polosukhin. Attention is all you need. In *Advances in Neural Information Processing Systems*, 2017.

P. Veličković, G. Cucurull, A. Casanova, A. Romero, P. Liò, and Y. Bengio. Graph Attention Networks. *International Conference on Learning Representations*, 2018.

O. Vinyals, M. Fortunato, and N. Jaitly. Pointer networks. In *Advances in Neural Information Processing Systems*, 2015.

R. J. Williams. Simple statistical gradient-following algorithms for connectionist reinforcement learning. *Machine Learning*, 8(3-4):229–256, 1992.

R. J. Williams and J. Peng. Function optimization using connectionist reinforcement learning algorithms. *Connection Science*, 3(3):241–268, 1991.

Y. Yu, J. Chen, T. Gao, and M. Yu. DAG-GNN: DAG structure learning with graph neural networks. In *ICML*, 2019.

K. Zhang and A. Hyvärinen. On the identifiability of the post-nonlinear causal model. In *Conference on Uncertainty in Artificial Intelligence*, 2009.

K. Zhang, J. Peters, D. Janzing, and B. Schölkopf. Kernel-based conditional independence test and application in causal discovery. In *Conference on Uncertainty in Artificial Intelligence*, 2012.

X. Zheng, B. Aragam, P. Ravikumar, and E. P. Xing. DAGs with NO TEARS: Continuous optimization for structure learning. In *Advances in Neural Information Processing Systems*, 2018.

B. Zoph and Q. V. Le. Neural architecture search with reinforcement learning. In *ICLR*, 2017.

APPENDIX

A   ALTERNATIVE DECODERS

We briefly describe the NN based decoders for generating binary adjacency matrices:

- Single layer decoder:

$$g_{ij}(W_1, W_2, u) = u^T \tanh(W_1 enc_i + W_2 enc_j),$$

  where $W_1, W_2 \in \mathbb{R}^{d_h \times d_e}$, $u \in \mathbb{R}^{d_h \times 1}$ are trainable parameters and d_h denotes the hidden dimension associated with the decoder.

- Bilinear decoder:

$$g_{ij}(W) = enc_i^T W enc_j,$$

  where $W \in \mathbb{R}^{d_e \times d_e}$ is a trainable parameter.

- Neural Tensor Network (NTN) decoder (Socher et al., 2013):

$$g_{ij}(W^{[1:K]}, V, b) = u^T \tanh \left(enc_i^T W^{[1:K]} enc_j + V[enc_i^T, enc_j^T]^T + b \right),$$

  where $W^{[1:k]} \in \mathbb{R}^{d_e \times d_e \times K}$ is a tensor and the bilinear tensor product $enc_i^T W^{[1:K]} enc_j$ results in a vector with each entry being $enc_i^T W^{[k]} enc_j$ for $k = 1, 2, \ldots, K$, $V \in \mathbb{R}^{K \times 2d_e}$, $u \in \mathbb{R}^{K \times 1}$, and $b \in \mathbb{R}^{K \times 1}$.

- Transformer decoder uses the multi-head attention module to obtain the decoder outputs $\{dec_i\}$, followed by a feed-forward NN whose weights are shared across all dec_i (Vaswani et al., 2017). The output consists of d vectors in $\mathbb{R}^d$ which are treated as the row vectors of a $d \times d$ matrix. We then pass each element of this matrix into sigmoid functions and sample a binary adjacency matrix accordingly.

Table 5 provides the empirical results on linear-Gaussian data models with 12-node graphs and unit variances (see Section 6.1 for more details on this data generating procedure). In our implementation, we pick $d_e = 64$ as the dimension of the encoder output, $d_h = 16$ for the single layer decoder, and $K = 2$ for the NTN decoder. We find that single layer decoder performs the best, possibly because it has less parameters and is easier to train to find better DAGs, while the Transformer encoder has provided sufficient interactions amongst variables to capture the causal relationships.

Table 5: Empirical results of different decoders on linear-Gaussian data models with 12-node graphs

		Single layer	Transformer	Bilinear	NTN
Linear-Gaussian	FDR	0 ± 0	0.67 ± 0.07	0.07 ± 0.13	0.12 ± 0.14
	TPR	1 ± 0	0.32 ± 0.09	0.95 ± 0.08	0.90 ± 0.11
	SHD	0 ± 0	38.2 ± 3.12	4.00 ± 7.04	7.40 ± 8.52

B   EQUIVALENCE OF PROBLEMS (1) AND (6)

Proof of Proposition 1. Let $\mathcal{G}$ be a solution to problem (1). Then we have $\mathcal{S}^* = \mathcal{S}(\mathcal{G})$ and $\mathcal{G}$ must be a DAG due to the hard acyclicity constraint. Assume that $\mathcal{G}$ is not a solution to problem (6), which indicates that there exists a directed graph $\mathcal{G}'$ (with binary adjacency matrix A') so that

$$\mathcal{S}^* > \mathcal{S}(\mathcal{G}') + \lambda_1 \mathbf{I}(\mathcal{G}' \notin \mathsf{DAGs}) + \lambda_2 h(A'). \tag{8}$$

Clearly, $\mathcal{G}'$ cannot be a DAG, for otherwise we would have a DAG that achieves a lower score than the minimum $\mathcal{S}^*$. By our assumption, it follows that

$$\text{r.h.s. of Eq. (8)} \geq \mathcal{S}_L + \lambda_1 + \lambda_2 h_{\min} \geq \mathcal{S}_U,$$

which contradicts the fact that $\mathcal{S}_U$ is an upper bound on $\mathcal{S}^*$.

For the other direction, let $\mathcal{G}$ be a solution to problem (6) but not a solution to problem (1). This indicates that either $\mathcal{G}$ is not a DAG or $\mathcal{G}$ is a DAG but has a higher score than the minimum score, i.e., $\mathcal{S}(\mathcal{G}) > \mathcal{S}^*$. The latter case clearly contradicts the definition of the minimum score. For the former case, assume that some DAG $\mathcal{G}'$ achieves the minimum score. Then plugging $\mathcal{G}'$ into the negative reward, we can get the same inequality in Eq. (8) since both penalty terms are zeros for a DAG. This then contradicts the assumption that $\mathcal{G}$ minimizes the negative reward. $\qquad\square$

C IMPLEMENTATIONS DETAILS

We use existing implementations of causal discovery algorithms in comparison, listed below:

- ICA-LiNGAM (Shimizu et al., 2006) assumes linear non-Gaussian additive model for data generating procedure and applies independent component analysis method to recover the weighted adjacency matrix, followed by thresholding on the weights before outputting the inferred graph. A Python implementation is available at the first author's website `https://sites.google.com/site/sshimizu06/lingam`.

- GES and PC: we use the fast greedy search implementation of GES (Ramsey et al., 2017) which has been reported to outperform other techniques such as max-min hill climbing (Han et al., 2016; Zheng et al., 2018). Implementations of both methods are available through the `py-causal` package at `https://github.com/bd2kccd/py-causal`, written in highly optimized Java codes.

- CAM (Peters et al., 2014) decouples the causal order search among the variables from feature or edge selection in a DAG. CAM also assumes additive noise as in our work, with an additional condition that each function is nonlinear. Codes are available through the CRAN R package repository at `https://cran.r-project.org/web/packages/CAM`.

- NOTEARS (Zheng et al., 2018) recovers the causal graph by estimating the weighted adjacency matrix with the least squares loss and the smooth characterization for acyclicity constraint, followed by thresholding on the estimated weights. Codes are available at the first author's github repository `https://github.com/xunzheng/notears`. We also re-implement the augmented Lagrangian method following the same updating rule on the Lagrange multiplier and the penalty parameter in Tensorflow, so that the augmented Lagrangian at each iteration can be readily minimized without the need of obtaining closed-form gradients. We use this implementation in Sections 6.2 and 6.3 when the objective function and/or the acyclicity constraint are modified.

- DAG-GNN (Yu et al., 2019) formulates causal discovery in the framework of variational autoencoder, where the encoder and decoder are two shallow graph NNs. With a modified smooth characterization on acyclicity, DAG-GNN optimizes a weighted adjacency matrix with the evidence lower bound as loss function. Python codes are available at the first author's github repository `https://github.com/fishmoon1234/DAG-GNN`.

- GraN-DAG (Lachapelle et al., 2019) uses feed-foward NNs to model each causal relationship and chooses the sum of all product paths between variables x_i and x_j as the (i, j)-th element of an equivalent weighted adjacency matrix. GraN-DAG uses the same smooth constraint from Zheng et al. (2018) to find a DAG that maximizes the log-likelihood of the observed samples. Codes are available at the first author's github repository `https://github.com/kurowasan/GraN-DAG`.

Our implementation is based on an existing Tensorflow implementation of neural combinatorial optimizer, which is available at `https://github.com/MichelDeudon/neural-combinatorial-optimization-rl-tensorflow`. We add an entropy regularization term, and modify the reward and decoder as described in Section 4 and Section 5.1.

D FURTHER EXPERIMENT DETAILS AND RESULTS

D.1 EXPERIMENT 1 IN SECTION 6.1

We replace the feed-forward NNs with linear functions in GraN-DAG and obtain similar experimental results as NOTEARS (FDR, TPR, SHD): 0.05 ± 0.04, 0.93 ± 0.06, 3.2 ± 2.93 and 0.05 ± 0.04, 0.95 ± 0.03, 2.40 ± 1.85 for LiNGAM and linear-Gaussian data models, respectively.

We conduct additional experiments with linear models where the noise variances are uniformly sampled according to $\mathrm{Unif}([0.5, 2])$. Results are given in Table 6.

Table 6: Empirical results on LiNGAM and linear-Gaussian data models with 12-node graphs and different noise variances

		RL-BIC	RL-BIC2	PC	GES	ICA-LiNGAM	CAM	NOTEARS	DAG-GNN	GraN-DAG
	FDR	0.29 ± 0.12	0.09 ± 0.06	0.57 ± 0.10	0.59 ± 0.13	0 ± 0	0.70 ± 0.07	0.08 ± 0.10	0.14 ± 0.07	0.71 ± 0.10
LiNGAM	TPR	0.77 ± 0.15	0.94 ± 0.03	0.28 ± 0.06	0.27 ± 0.10	1 ± 0	0.45 ± 0.12	0.94 ± 0.07	0.91 ± 0.04	0.25 ± 0.09
	SHD	14.4 ± 7.17	4.00 ± 2.61	30.4 ± 4.13	32.0 ± 5.18	0 ± 0	41.6 ± 3.32	3.20 ± 3.97	6.60 ± 1.02	38.7 ± 4.86
	FDR	0.36 ± 0.07	0.10 ± 0.07	0.54 ± 0.10	0.61 ± 0.14	0.67 ± 0.05	0.65 ± 0.10	0.07 ± 0.09	0.12 ± 0.04	0.71 ± 0.12
Linear-Gaussian	TPR	0.68 ± 0.09	0.93 ± 0.04	0.29 ± 0.05	0.26 ± 0.11	0.75 ± 0.06	0.51 ± 0.14	0.95 ± 0.06	0.94 ± 0.04	0.21 ± 0.08
	SHD	18.8 ± 3.43	4.60 ± 3.07	30.0 ± 2.83	32.2 ± 5.42	49.0 ± 4.82	37.8 ± 6.31	3.00 ± 3.58	5.40 ± 2.06	39.6 ± 5.85

D.2 EXPERIMENT 2 IN SECTION 6.2

To remove 'outlier' samples with large values that may cause computation issues for quadratic regression, we sort the samples in ascending order according to their ℓ_2-norm and then pick the first $3,000$ samples for causal discovery.

We use a similar idea from GraN-DAG to build an equivalent weighted adjacency matrix for NOTEARS. Take the first variable x_1 for example. We first expand the rest variables $x_2, \ldots, x_d$ to contain both first- and second-order features: $x_2, \ldots, x_d, x_2 x_3, \ldots, x_i x_j, \ldots, x_{d-1} x_d$ with $i, j = 2, \ldots, d$ and $i \leq j$. There are in total $d(d-1)/2$ terms and we use $\mathbf{x}_1$ to denote the vector that concatenates these feature terms. Correspondingly, we use c_i and c_{ij} to denote the coefficients associated with these features and $\mathbf{c}_1$ to denote the concatenating vector of the coefficients. Notice that the variable x_l, $l \neq 1$ affects x_1 only through the terms x_l, $x_i x_l$ with $i \leq l$, and $x_l x_j$ with $j > l$. Therefore, an equivalent weighted adjacency matrix W lying in $\mathbb{R}^{d \times d}$ can be constructed with the $(l, 1)$-th entry $W_{l1} := |c_l| + \sum_{i=2}^{l} |c_{il}| + \sum_{j=l+1}^{d} |c_{lj}|$; in this way, $W_{l1} = 0$ implies that x_l has no effect on x_1. The least squares term, corresponding to variable x_1, in the loss function will become $\sum_{k=1}^{D} (x_1^k - \mathbf{c}_1^T \mathbf{x}_1^k)^2$ where D is total number of samples. In summary, we have the following optimization problem

$$\min_{\mathbf{c}_1, \mathbf{c}_2, \ldots, \mathbf{c}_d} \quad \sum_{i=1}^{d} \sum_{k=1}^{D} (x_i^k - \mathbf{c}_i^T \mathbf{x}_i^k)^2$$
$$\text{subject to} \quad \mathrm{trace}\left(e^{W \circ W}\right) - d = 0,$$

where $\circ$ denotes the Hadamard product. The problem has $(d-1)d^2/2$ parameters to optimize, while the original NOTEARS optimizes d^2 parameters. We solve this problem with augmented Lagrangian method where at each iteration the augmented Lagrangian is minimized by the stochastic method Adam (Kingma and Ba, 2014) with Tensorflow. The Lagrangian multiplier and the penalty parameter is updated in the same fashion as in the original NOTEARS.